

# Monochromatic Image Analysis of Elastohydrodynamic Lubrication Film Thickness by Fringe Intensity Computation

Siyoul Jang\*

*School of Mechanical & Automotive Engineering, Kookmin University,  
861-1, Jungnung-dong, Sungbuk-gu, Seoul 136-702, Korea*

Point contact film thickness in elastohydrodynamic lubrication (EHL) is analyzed by image processing method for the images from an optical interferometer with monochromatic incident light. Interference between the reflected lights both on half mirror  $Cr$  coating of glass disk and on super finished ball makes circular fringes depending on the contact conditions such as sliding velocity, applied load, viscosity-pressure characteristics and viscosity of lubricant under ambient pressure. In this situation the film thickness is regarded as the difference of optical paths between those reflected lights, which make dark and bright fringes with monochromatic incident light. The film thickness is computed by numbering the dark and bright fringe orders and the intensity (gray scale image) in each fringe regime is mapped to the corresponding film thickness. In this work, we developed a measuring technique for EHL film thickness by dividing the image patterns into two typical types under the condition of monochromatic incident light. During the image processing, the captured image is converted into digitally formatted data over the contact area without any loss of the image information of interferogram and it is also interpreted with consistency regardless of the observer's experimental experience. It is expected that the developed image processing method will provide a valuable basis to develop the image processing technique for color fringes, which is generally used for the measurement of relatively thin films in higher resolution.

**Key Words :** Elastohydrodynamic Lubrication (EHL), Gray Scale Image, Monochromatic, Image Processing Method, Optical Interferometer

## 1. Introduction

Film thickness is one of the most important measurands in analyzing the characteristics of lubricant under high load and shear contact conditions (that is, EHL regime), where most failures happen. Under the assumption of continuum mechanics, film thickness varies only as a function of lubricant viscosity of ambient pressure if other contact conditions such as contact geome-

try, applied load and contact velocity are invariables. Therefore, measuring both thicknesses and patterns of fluid film in EHL regime provides a direct information of lubricant properties especially for load capacity and shear resistance.

There are several experimental methods for measuring fluid film thickness. Electrical, mechanical and optical methods have been developed but in many cases optical method for measuring the EHL film thickness is the most useful in-situ method, because it gives high resolution of film thickness up to  $0.01 \mu\text{m}$  and broad measuring scope over all contact area. However, this method needs high transparent glass on either side of the contact components, which sometimes prevents optical method from being applied to real mechanical components. In spite of this disadvantage,

---

\* E-mail : jangs@kookmin.ac.kr

TEL : +82-2-910-4831; FAX : +82-2-910-4839

School of Mechanical & Automotive Engineering, Kookmin University, 861-1, Jungnung-dong, Sungbuk-gu, Seoul 136-702, Korea. (Manuscript Received March 19, 2003; Revised August 21, 2003)

it is still a popular method for measuring the EHL film thickness because it provides more information about the EHL phenomena than other methods.

Optical method for measuring the fluid film thickness in EHL is divided into two ways according to the magnitudes of wavelengths of the incident lights. White incident light which contains all frequencies of visible light makes colorful fringes, while monochromatic incident light has only dark and bright fringes over the contact area. Therefore, the interpretation of fringe patterns by white incident light differs from that by monochromatic incident light (Cann, 1996; Gustafson, 1997). The image processing method for white incident light uses more parameters so that it is applicable to determining thin fluid film thickness of about  $0.01 \sim 1.0 \mu\text{m}$  with high resolution. In the case of monochromatic incident light, the image processing method uses only dark and bright information of the fringe patterns. Therefore, it is useful for measuring relatively thick film thickness of about  $0.15 \sim 2.0 \mu\text{m}$  (Bassani, 1996). However, the image processing method using white incident light should be based on the results of monochromatic incident light, (Krupka, 1997) and this is the reason why the monochromatic image processing method should be performed prior to the color image processing analysis.

In this work, image processing method using a monochromatic incident light is investigated for the color image processing method which will improve the objectiveness and consistency of interpretation of measured the EHL-image data.

## 2. Experimental Apparatus and Phase Change Computation

### 2.1 Experimental apparatus

The experimental apparatus for measuring the film thickness is divided into two parts as shown in Fig. 1. One is the optical part which consists of an illuminator, collimator, microscope and an image capture device. The other is the mechanical part which consists of a super-finished steel ball, *Cr* coated quartz glass (half mirror) and driving

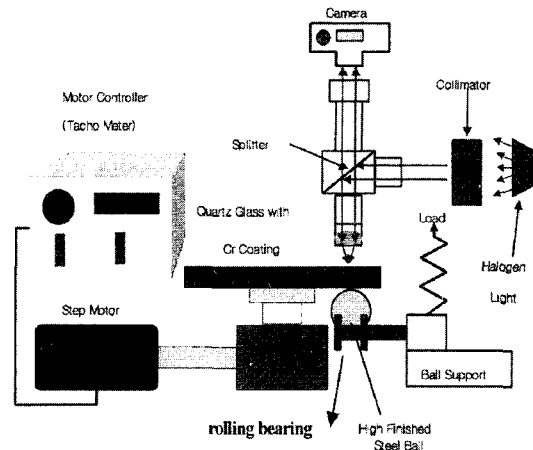


Fig. 1 Schematic diagram of EHL film measurement

components. In this mechanical part, circular point contact between the quartz glass and the steel ball physically occurs and the image of contact behavior is viewed through the microscope. The incident light from the halogen illuminator is screened with a green light filter ( $\lambda=530 \text{ nm}$ , bandwidth  $20 \text{ nm}$ ) in order to make monochromatic images and then enters the collimator. The incident light which goes through the collimator is paralleled and splitted in two directions. One direction is to the steel ball where the contact behavior occurs and the other is to the eyepiece of the microscope.

By adjusting the layer thickness of *Cr* for the highest contrast of fringes, the incident light to the contact point is reflected by 25% on the *Cr* coated layer and the rest of it is reflected by 25% on the super finished ball ( $nm$  scale roughness). The interference between the reflected lights from the super finished ball and the *Cr* coated layer makes circular dark and bright fringes which are stored by the image capturing devices. In this experiment the image is stored in 35 mm film and digitized with a film scanner in order to save the color information in all pixels. This procedure expels the observer's subjectiveness and provides a higher resolution of manageable digital data compared to the observation made by the naked eye only.

In order to precisely examine the interference images, it is most important to remove all the

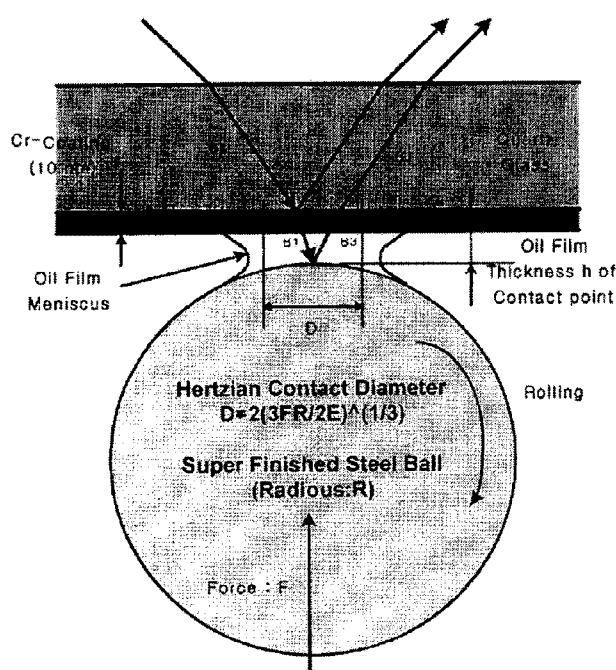


Fig. 2 Reflected beams on half mirror of Cr coating surface and steel ball surface

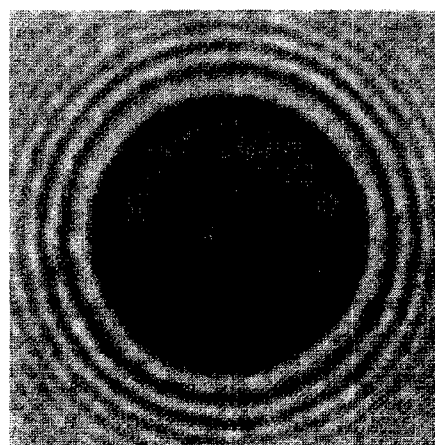
small stains and vibrations that can cause disturbances in the captured images. This is the reason why the scanning of the fringe pattern is greatly influenced by micro-scale agitation of the mechanical part in the developed apparatus. Furthermore, monochromatic image uses only dark and bright intensities in the fringes and this requires more careful operation (Johnston, 1991).

The elastic modulus and Poisson's ratio of steel ball and quartz glass are  $E_b = 207 \times 10^9 \text{ N/m}^2$ ,  $\nu_b = 0.30$  and  $E_d = 76 \times 10^9 \text{ N/m}^2$ ,  $\nu_d = 0.25$ , respectively. The Cr coating is evenly sputtered on the quartz glass to 100 Å thickness and the steel ball is super finished in order not to interrupt the film formation of sub-micrometer scale thickness (Fig. 2).

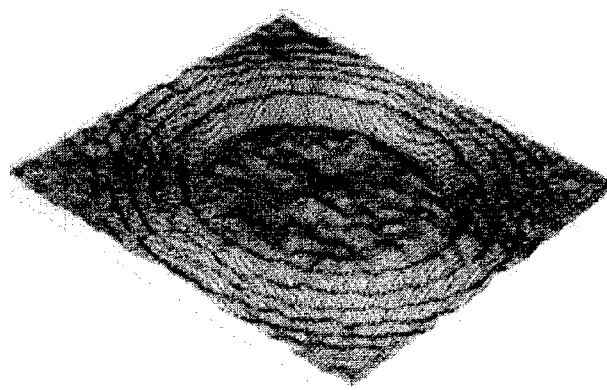
## 2.2 Computation of phase change in the reflection

The fringe pattern created by a green monochromatic incident light is shown in Fig. 3 under the static condition. The fringe pattern has the same feature as a Newton ring and the optical path is computed by numbering the fringe orders Moller (1988), Born (1997).

By using the parameters such as fringe order  $K$ , reflective intensity  $n$ , wavelength  $\lambda$  and phase



(a) Static monochromatic interferogram for Hertzian contact of 5 N static load



(b) Intensity modulation of interferogram by monochromatic incident light under Hertzian contact condition (5 N static load)

Fig. 3 EHL Interferogram of static contact condition

change  $\psi$ , the gap distance between the steel ball and the glass is calculated by the following method:

For dark fringes

$$h = \left( K + \frac{1}{2} + \frac{\psi}{2\pi} \right) \frac{\lambda}{2n}, \quad (K=0, 1, 2, 3, \dots) \quad (1)$$

and for bright fringes

$$h = \left( K + \frac{\psi}{2\pi} \right) \frac{\lambda}{2n}, \quad (K=1, 2, 3, \dots) \quad (2)$$

The wavelength of incident light and the lubricant refractive index are 530 nm and  $n=1.40$ , respectively and the fringe orders can be counted from the captured image. In order to compute the film thickness (Opt formula in Fig. 5) by Eqs. (1) and (2), the magnitude of phase change,  $\psi$ ,

which occurs on the quartz glass should be obtained with all the above values. Although electronic microscope can accurately measure the phase change value, it is easily computed by comparing the experimental data with the Hertzian contact theory that clearly explains the concentrated point contact behavior. The theoretical film gap outside of the contact area is described by Eq. (3) and is compared with the intensity values of the fringes at the same geometrical location :

$$h = \frac{aP_H}{E'} \left[ \left( \frac{r^2}{a^2} - 2 \right) \cos^{-1} \left( \frac{a}{r} \right) + \sqrt{\frac{r^2}{a^2} - 1} \right] \quad (3)$$

The Hertzian contact radius is described by Eq. (4)

$$a = \sqrt[3]{1.5FR/E'} \quad (4)$$

where  $F$  is the applied normal force,  $R$  is the radius of the steel ball and  $E'$  is the equivalent elastic modulus given by

$$E' \approx 2 \left[ (1 - \nu_1^2)/E_1 + (1 - \nu_2^2)/E_2 \right]^{-1} \quad (5)$$

The maximum contact pressure is then expressed as follows :

$$P_H = 1.5F/\pi a^2 \quad (6)$$

By comparison of the results given by Eqs. (1), (2) and (3), the phase change value is obtained for the given characteristics of coating layer on the glass. The intensities related with film thickness are sampled in four directions (where  $a, b, c, d$  in Fig. 4) and the mean values along the same contact radius are computed from the lined pixels in each direction. The mean values of the four directions are obtained from Eqs. (1) and (2) and compared with the theoretical film thickness given by Eq. (3). The difference between the results obtained by optical measurement and Hertzian analyses is minimized by using the least squares method and then the phase change value,  $\psi$ , is computed. The optimized film thickness obtained by optical and Hertzian analyses are shown in Fig. 5, where the computed value of the phase change is  $-0.55$ . By using this value, all the intensities of the captured image are converted into physical values of film thickness with

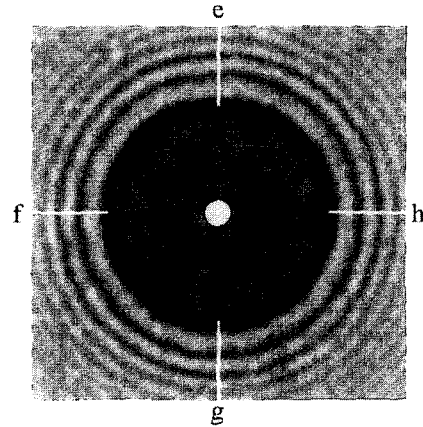


Fig. 4 Directions of selected pixels for determining the phase change  $\psi$

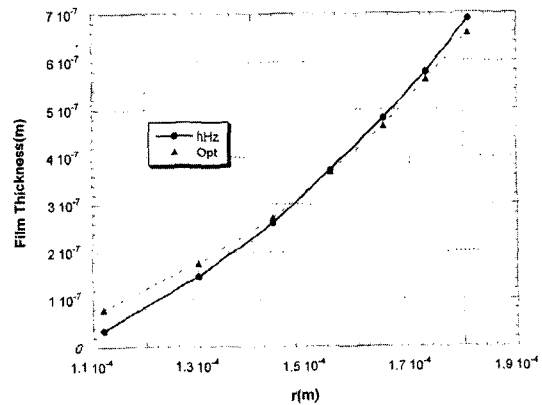


Fig. 5 Thickness values optimised with least squares method for Hertz (hHz) and optical (Opt) formulas

Eqs. (1) and (2) over the entire contact area. This process is necessary whether the image is monochromatic or chromatic, because the relationship between the EHL film thickness and color or intensity must be set up before the intensity or color parameters are converted into film thickness values.

### 3. Monochromatic Image Processing of EHL Interferogram by Imaginary Elliptic Circling Method

The purposes of image processing for film

thickness measurement in EHL are to remove observer's subjectivity and to obtain the consistency of interpretation for the captured image that might be differently interpreted depending on the observers. The typical fringe pattern obtained by monochromatic incident light is shown in Fig. 6 (type I). The first thing in monochromatic image processing procedure is to find the center point (or pixel) of the contact area with imaginary elliptic circling. In order to minimize the observer's subjectivity in selecting the center point by naked eye, eight points (pixels from  $a$  to  $h$ ) around the first and second bright fringes are selected. Each point on the first and second bright fringes is connected into a line ( $a-b$ ,  $c-d$ ,  $e-f$ ,  $g-h$ ) and the pixel locations that have the minimum intensity on each line are searched. By con-

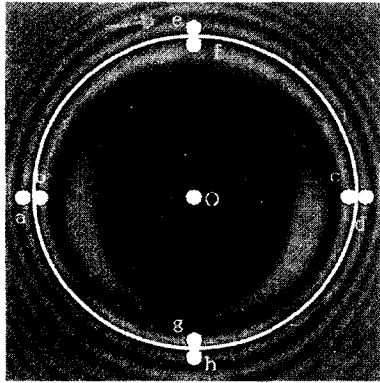


Fig. 6 Points selected for determining the center ( $O$ ) of contact regime (type I)

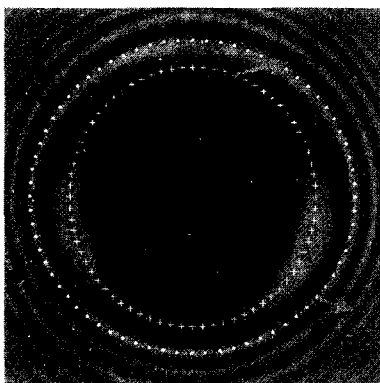


Fig. 7 Imaginary elliptical circles for the boundary points of horseshoe shaped area

necting these pixels, the imaginary elliptic circle ( $W1$ ) and the its center ( $O$ ) are constructed. Further removal of subjectivity in selecting 8 pixels ( $a$ ,  $b$ ,  $c$ ,  $d$ ,  $e$ ,  $f$ ,  $g$ ,  $h$ ) is obtained by checking if each elliptic imaginary circles (Fig. 7,  $B1$ ,  $B2$ ) in the first and second bright fringes are centered at one pixel location,  $O$ .

With the imaginary elliptic circle  $B1$ , the boundary of the first bright fringe that looks like a horse shoe shaped in Hertzian contact region can be located. By using the symmetric feature of the fringe patterns in left and right sides (otherwise, the mechanical part of the experimental apparatus is not aligned correctly.), the minimum intensity locations  $N1$  and  $N2$  are selected on the elliptic circle  $B1$ . In order to fix the horse shoe shape of the first bright fringe, the minimum number of pixels are selected along the line connected between the points of center  $O$ , and imaginary elliptic circle  $B1$ , which makes the line  $D1$  shown in Fig. 8. In the same way of making line  $D1$ , two points on the imaginary elliptic circles  $B1$  and  $B2$  are connected by a line with the same center location of pixel  $O$ . The pixels of minimum intensity in each connected line between  $B1$  and  $B2$  make another imaginary elliptic circle  $D2$ . By locating the imaginary elliptic circle  $D2$ , the first bright fringe of horse shoe shape is determined on the digitized domain of the interference image. The successive bright or dark fringes are made by the circles centered at pixel  $O$  in the same way as

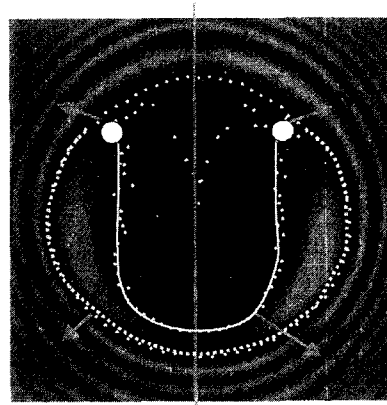


Fig. 8 Boundary points in the horseshoe shaped area for type I

explained above. The intensity values in the first bright fringe region are mapped into the values of film thickness, with which the film thickness in the successive fringe is also calculated. The difference of film thickness magnitude between the successive bright and dark fringes is given by Eq. (7) and the film thickness of each fringe is computed by Eqs. (1) and (2).

$$\Delta h = \frac{\lambda}{4n} \tag{7}$$

The linear conversion from intensity value into film thickness has 256 levels for every captured pixel and is described by the following equation :

$$h = \left( \frac{\Delta h}{I_{max} - I_{min}} \right) I, \quad (I_{min} < I < I_{max}) \tag{8}$$

where,  $I_{max}$  and  $I_{min}$  are the maximum and minimum intensities, respectively, that each pixel can have.

The assignment of film thickness by Eq. (8) is uniformly made over the Hertzian contact region in order to maximize all the information of the captured image as shown in Fig. 9. The matching pixels to be connected as a line are located on the imaginary elliptical circles  $D1$  and  $D2$  in the contact region and on the successive imaginary elliptical circles for the outer contact region. The number of pixels on each imaginary circle centered at pixel  $O$  is selected to be about 72 which is  $5^\circ$  apart.

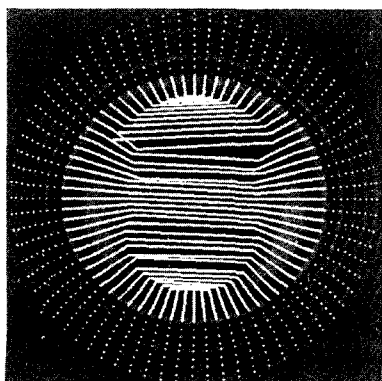


Fig. 9 Interferogram with determined points for the calculation of heights (type I)

Another typical pattern of interference image for the monochromatic incident light is shown in Fig. 10 (type II), where the first bright fringe is separated in the horseshoe-like region. The boundary of the first bright fringe should be made for the assignment of film thickness without any subjectivity. Looking at a certain portion of the imaginary elliptical circle,  $l_d$ , in Fig. 11, minimum intensity pixels that creates a new fringe region are found. The existence of a circular arc region (region of elliptical circle  $l_d$ ) between the pixels of minimum intensity is the major difference from the case of Fig. 6 (type I), where it does not show separated horseshoe feature. Therefore, both the functions of making the circular arc,  $l_d$ , and selecting the minimum intensity

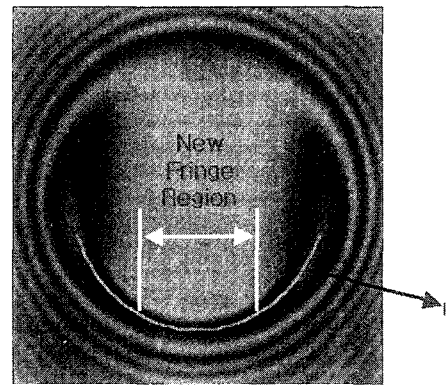


Fig. 10 EHL monochromatic interferogram (type II)

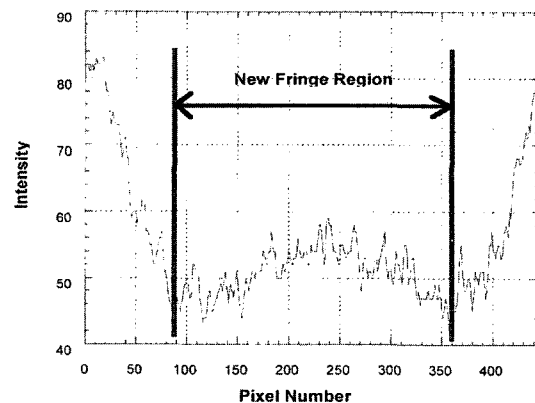


Fig. 11 Intensity of Fig. 10 solid line  $l_d$  (new fringe region, type II)

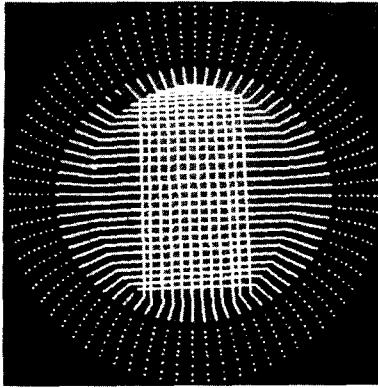


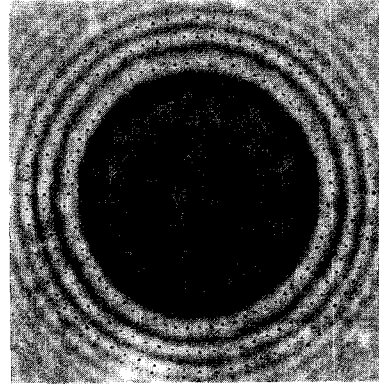
Fig. 12 EHL monochromatic interferogram with determined points for calculation of heights (type II)

pixels in the circular arc are added to the case of Fig. 6. Pixels for the conversion of intensity values to film thickness are selected as shown in Fig. 12, which has different shape from that of Fig. 9 due to the existence of the circular arc  $l_a$ , between the first bright fringes. Other patterns of dimple due to large sliding to rolling ratios and bump due to external particles are not considered in this monochromatic image processing method, because they are the concerns of chromatic interferograms with finer resolution.

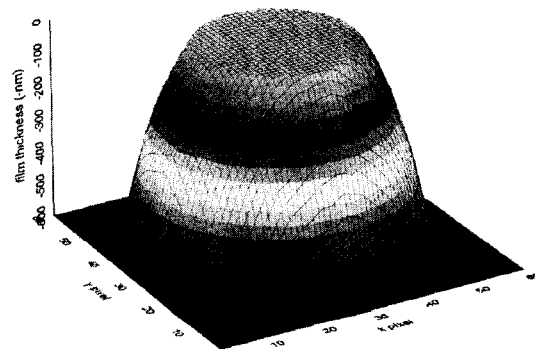
The developed imaginary elliptic circling method can determine the elliptic circles exactly on dark and bright fringes by selecting eight distinct pixels of maximum and minimum intensities. Even the observer's subjectivity in selecting these eight pixels can be minimized by deciding the successive elliptic circles on the next dark and bright fringes. Therefore, the monochromatic imaging processing method of EHL film thickness developed in this work can provide the film thickness with high accuracy over the entire contact region as much as the digitizing capacity of the film scanner can offer. The digitization for all the pixels in the contact region provides higher repeatability and objectivity compared with the results obtained by naked eye observation.

#### 4. Results

In order to verify the conversion theory of



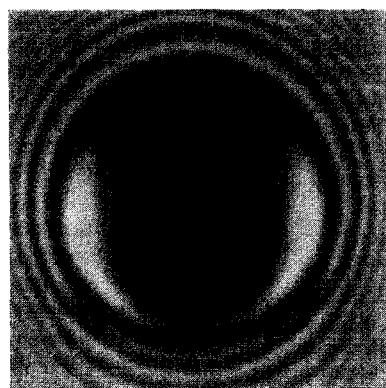
(a) Monochromatic interferogram of Hertzian contact with determined points for calculation of heights



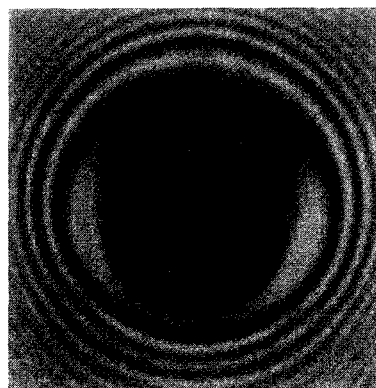
(b) 3-D mesh surface plot of static contact

Fig. 13 Film thickness of monochromatic EHL interferogram under static condition

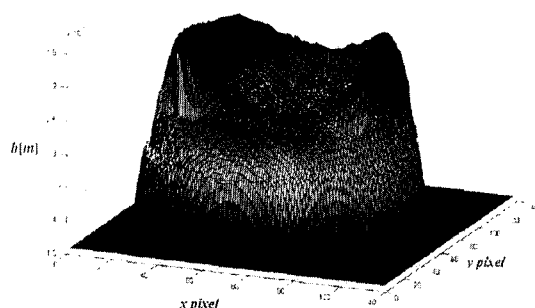
fringe intensity into film thickness, static loading condition is tested for its simplicity and easy comparison with the Hertzian theory. On the fringe pattern under the static loading condition of 5 N, pixels for the computation of film thickness are selected as shown in Fig. 13(a). In order to be more accurate, 72 directions are selected for minimum and maximum intensities along the same order of fringe, and the center location of the contact region is computed from these values. 72 pixels are located on each dark and bright fringe and more circles are made in the Hertzian contact region. The phase shift value,  $\psi$ , is computed by comparison of the pixel intensities with the theoretical values given by Eqss. (1), (2) and (3). According to the fringe order and brightness of the pixels, the film thicknesses are assigned for the static contact image. The image-processed



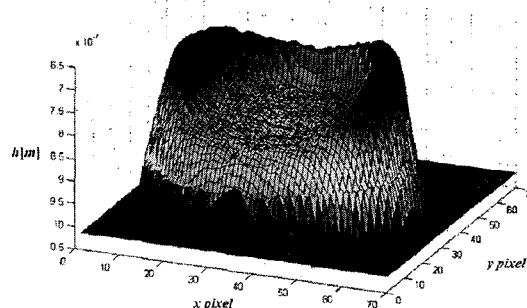
(a) Monochromatic EHL interferogram of film thickness (10 N of applied load, 0.034 m/s of rolling contact speed)



(c) Monochromatic EHL interferogram of film thickness (10 N of applied load, 1.01 m/s of rolling contact speed)



(b) Computed film thickness of iterferogram (a) (10 N of applied load, 0.034 m/s of rolling contact speed)



(d) Computed film thickness of monochromatic EHL iterferogram (c), (10 N of applied load, 1.01 m/s of rolling contact speed)

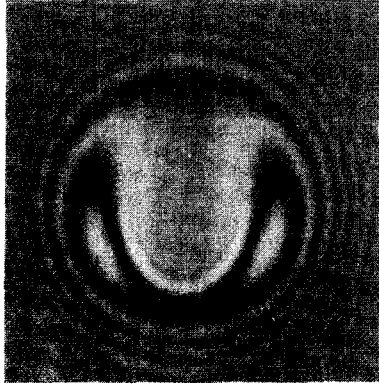
**Fig. 14** Monochromatic images and film thickness of two patterns under rolling contact condition (type I)

film thickness for the static contact condition is shown in Fig. 13(b).

The lubricant viscosity at atmospheric condition in our experiment is 0.0411 Pa·s and the applied load of 10 N is imposed in order to make the EHL iterferogram. The test is performed at room temperature of 20°C. The rolling velocities are selected from 0.034 m/s to 1.20 m/s. The steel ball is super-finished in order to remove any roughness and bumps that may interrupt the film formation. Because the monochromatic incident light can generate an interference image of relatively thick film up to 3  $\mu\text{m}$ , the rolling velocity is set to be relatively high to get a thick film formation in this experiment. The fringe patterns under the sliding condition of 0.034 m/s and 1.01 m/s with applied force of 10 N are shown

in Fig. 14(a) and (c) for type I case. The film thickness from these interference images are computed by the imaginary elliptic circling method developed in our work. The converted film thicknesses are shown in Fig. 14(b) and (d). For type II, rolling speed of 0.157 m/s and 1.20 m/s under the same applied load of 10 N are applied. The interference images given in Fig. 14(a) and (c) show different images from Fig. 15(a) and (c). In this case, the interference image has a disconnected horse-shoe shape, where the film thickness is computed by the modified imaginary elliptic circling method and the film thicknesses are shown in Fig. 15(b) and (d), respectively. Looking at the minimum film thickness in each graph of film thickness for the 10 N applied load, it shows an increasing tendency as the rolling

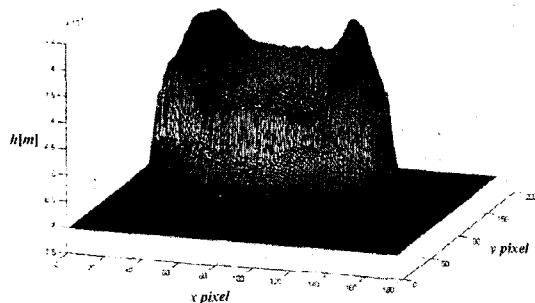




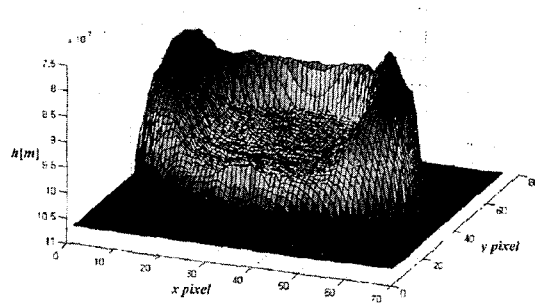
(a) EHL monochromatic interferogram of film thickness (10 N of applied load, 0.157 m/s of rolling contact speed)



(c) EHL monochromatic interferogram of film thickness (10 N of applied load, 1.20 m/s of rolling contact speed)



(b) Computed film thickness of monochromatic interferogram (a) (10 N of applied load, 0.157 m/s of rolling contact speed)



(d) Computed film thickness of monochromatic interferogram (c) (10 N of applied load, 1.20 m/s of rolling contact speed)

**Fig. 15** Monochromatic images and film thickness of two patterns under dynamic condition (type II)

contact speed rises, namely  $\sim 150$  nm (0.034 m/s),  $\sim 350$  nm (0.034 m/s),  $\sim 650$  nm (1.01 m/s),  $\sim 750$  nm (1.20 m/s). This behavior agrees well with the theoretical EHL investigations by many other works (Hamrock, 1994).

## 5. Conclusion

The film thickness under monochromatic incident light is measured up to  $\sim 1.0$   $\mu\text{m}$  range by the optical interference method, where the film thickness is regarded as the difference of optical path between the incident and the reflected lights. Two typical patterns of interference images of rolling EHL contact are found under the condition of rolling contact. In order to accurately interpret the monochromatic image, imaginary

elliptic circling method that makes the conversion of fringe intensity into film thickness is developed for general patterns of EHL film thickness. The developed technique removes the observer's subjectiveness, allows good repeatability and obtains the two-dimensional film thickness over the entire contact area. It is expected that the developed image processing method will provide a valuable basis to develop the image processing technique of color fringes as long as the calibration of film thickness is concerned.

## Acknowledgment

This work was supported by grant No. 2000-1-30400-005-3 from the Basic Research Program of the Korea Science & Engineering Foundation.

## References

- Bassani, R. and Ciulli, E., 1996, "Lubricant Film Thickness and Shape Using Interferometry and Image Processing," *Elastohydrodynamics-96 Fundamentals and Application in Lubrication and Traction*, Elsevier, Amsterdam.
- Born M. and Wolf, E., *Principles of Optics*, 1997, Cambridge University Press.
- Cann, P. M., Spikes, H. and Hutchingson, J., 1996, "The Development of a Space layer Imaging Method (SLIM) for Mapping Elastohydrodynamic Contacts," *Tribology Transactions*, Vol. 39, pp. 915~921.
- Giancoli, D. C., 1999, *General Physics*, 3<sup>rd</sup> Edition, Prentice-Hall.
- Gustafsson, L., Hoglund, E. and Marklund, O., 1997, "Measuring Lubricant Film Thickness with Image Analysis," *Journal of Engineering Tribology*, Vol. 204, pp. 199~205.
- Hamrock, B. J., 1994, *Fundamentals of Fluid Film Lubrication*, McGraw-Hill.
- Johnston, G. J., Wayte, R. and Spikes, H. A., 1991, "The Measurement and Study of Very Thin Lubricant Films in Concentrated Contact," *Tribology Transactions*, Vol. 34, pp. 187~194.
- Krupka, M. et al., 1997, "Elastohydrodynamic Lubrication Film Shape — Comparison Between Experimental and Theoretical Results," *Tribology for Energy Conservation*, Elsevier, Amsterdam.
- Moller, K. D., 1997, *Optics*, University Science Books.
- Zhang, X. and Wandell, B. A., 1998, "Color Image Fidelity Metrics Evaluated Using Image Distortion Maps," *Elsevier Preprint*.